

Dose dependent pharmacokinetics, tissue distribution, and anti-tumor efficacy of a humanized monoclonal antibody against DLL4 in mice

Amrita V Kamath^{1,*}, Victor Yip¹, Priyanka Gupta¹, C Andrew Boswell¹, Daniela Bumbaca¹, Peter Haughney¹, Joni Castro², Siao Ping Tsai², Glenn Pacheco³, Sarajane Ross³, Minhong Yan⁴, Lisa A Damico-Beyer¹, Leslie Khawli^{1,†}, and Ben-Quan Shen^{1,*}

¹Department of Preclinical and Translational Pharmacokinetics and Pharmacodynamics; Genentech, Inc; South San Francisco, CA USA; ²Department of Biochemical and Cellular Pharmacology; Genentech, Inc; South San Francisco, CA USA; ³Department of Translational Oncology; Genentech, Inc; South San Francisco, CA USA;

⁴Department of Research Oncology; Genentech, Inc; South San Francisco, CA USA

[†]Current address: Keck School of Medicine; University of Southern California; Los Angeles, CA USA

Keywords: DLL4, antibody, pharmacokinetics, tissue distribution, cancer

Delta-like-4 ligand (DLL4) plays an important role in vascular development and is widely expressed on the vasculature of normal and tumor tissues. Anti-DLL4 is a humanized IgG1 monoclonal antibody against DLL4. The purpose of these studies was to characterize the pharmacokinetics (PK), tissue distribution, and anti-tumor efficacy of anti-DLL4 in mice over a range of doses. PK and tissue distribution of anti-DLL4 were determined in athymic nude mice after administration of single intravenous (IV) doses. In the tissue distribution study, radiolabeled anti-DLL4 (mixture of ¹²⁵Iodide and ¹¹¹Indium) was administered in the presence of increasing amounts of unlabeled anti-DLL4. Dose ranging anti-DLL4 anti-tumor efficacy was evaluated in athymic nude mice bearing MV522 human lung tumor xenografts. Anti-DLL4 had nonlinear PK in mice with rapid serum clearance at low doses and slower clearance at higher doses suggesting the involvement of target mediated clearance. Consistent with the PK data, anti-DLL4 was shown to specifically distribute to several normal tissues known to express DLL4 including the lung and liver. Maximal efficacy in the xenograft model was seen at doses ≥ 10 mg/kg when tissue sinks were presumably saturated, consistent with the PK and tissue distribution profiles. These findings highlight the importance of mechanistic understanding of antibody disposition to enable dosing strategies for maximizing efficacy.

Introduction

The NOTCH pathway is an important signaling system that influences cell proliferation, differentiation and death in a variety of tissue types.^{1–4} In mammals, the notch system consists of four single-pass transmembrane receptors, NOTCH1–4, and at least five membrane-anchored ligands, Jagged1 and 2, and Delta-like ligand (DLL)1, 3, and 4. Endothelial cells have been shown to express two of the receptors, NOTCH1 and NOTCH4, and all of the above ligands except for DLL3.^{5–7} Despite the multiple NOTCH ligands and receptors in the vascular system, DLL4 mediated NOTCH1 signaling appears to be an essential pathway for vascular development.⁴ Loss of a single DLL4 allele in mice

results in embryonic lethality due to severe vascular defects, emphasizing its essential role in regulating vessel formation.^{4,8–10} DLL4 was initially identified as an endothelium-specific notch ligand, and its activation of the NOTCH1 pathway occurs in response to angiogenic signals, including vascular endothelial growth factor (VEGF).^{4,8,11–13} This activation results in negative feedback causing downregulation of the VEGF receptor, VEGFR2, which restrains endothelial cell proliferation and sprouting.^{4,14,15} Blockade of DLL4-mediated NOTCH1 signaling causes excessive angiogenic sprouting and branching resulting in a chaotic vascular network with defective functions.^{4,14} Due to its essential role in angiogenesis, DLL4-NOTCH1 signaling has emerged as an attractive new target for anti-angiogenesis with

© Amrita V Kamath, Victor Yip, Priyanka Gupta, C Andrew Boswell, Daniela Bumbaca, Peter Haughney, Joni Castro, Siao Ping Tsai, Glenn Pacheco, Sarajane Ross, Minhong Yan, Lisa A Damico-Beyer, Leslie Khawli, and Ben-Quan Shen

*Correspondence to: Amrita V Kamath: Email: kamath.amrita@gene.com; Ben-Quan Shen: Email: shen.ben@gene.com

Submitted: 06/27/2014; Revised: 08/08/2014; Accepted: 08/16/2014

<http://dx.doi.org/10.4161/mabs.36107>

This is an Open Access article distributed under the terms of the Creative Commons Attribution-Non-Commercial License (<http://creativecommons.org/licenses/by-nc/3.0/>), which permits unrestricted non-commercial use, distribution, and reproduction in any medium, provided the original work is properly cited. The moral rights of the named author(s) have been asserted.

implications for cancer therapy. Previous therapies targeting NOTCH signaling such as gamma secretase inhibitors (GSIs) had major hurdles such as on-target toxicity in the gastrointestinal tract.^{4,16} As reviewed by Yan,⁴ GSIs block all NOTCH receptors, whereas selective inhibition of DLL4 appears to avoid gut toxicity as both DLL1 and DLL4 appear to be key ligands that mediate NOTCH signaling in the intestinal epithelium, therefore blocking DLL4 alone will not cause gastrointestinal toxicity. However, chronic blockade of DLL4 appears to have other safety concerns in preclinical models such as histopathological changes in the liver in mice, rats, and cynomolgus monkeys, and subcutaneous vascular lesions in rats.¹⁷

Anti-DLL4 is a phage-derived humanized immunoglobulin (Ig)G1 monoclonal antibody (mAb) that binds selectively to DLL4 and blocks its interaction with the NOTCH receptor.^{17,18} Anti-DLL4 cross-reacts with DLL4 proteins from multiple species, including mouse, rat, cynomolgus monkeys, and humans. In preclinical studies, treatment with anti-DLL4 resulted in a structurally chaotic and functionally defective tumor vasculature, as well as marked tumor growth inhibition. Anti-DLL4 also demonstrated an additive effect in combination with anti-VEGF therapy to further reduce tumor growth in mouse xenograft models. However, anti-DLL4 also showed significant safety concerns in preclinical models as previously reported by Yan et al.,¹⁷ and briefly described above as arising through chronic blockade of DLL4, highlighting the need for further evaluation of this molecule.

DLL4 is known to be widely expressed in the vasculatures of various normal tissues.¹⁹ Binding to the target in these tissues could significantly affect the pharmacokinetics (PK) of anti-DLL4. However, little information is available on whether anti-DLL4 would have any specific tissue distribution, and if so, what effect this might have on PK and anti-tumor activity. In this report, we investigated the PK, tissue distribution, and efficacy of anti-DLL4 in mice, as well as the dose-dependency of these measurements, to gain a better understanding of the characteristics of this antibody and inform further drug development efforts.

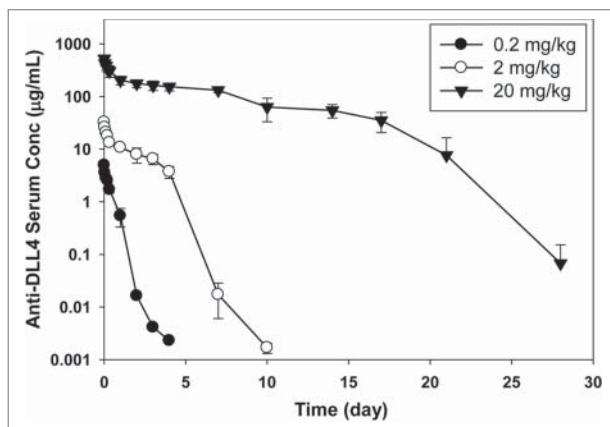


Figure 1. Anti-DLL4 serum concentration–time profiles in athymic nude mice after IV administration (average \pm SD, n = 3 per time point).

Table 1. Anti-DLL4 pharmacokinetic parameters in non-tumor bearing athymic nude mice

Parameter	0.2 mg/kg	2 mg/kg	20 mg/kg
Measured dose (mg/kg)	0.11	2.1	16.6
Cmax (μ g/mL)	5.0	32.5	524
AUCinf (day \cdot μ g/mL)	2.0	42	2014
CLtot (mL/day/kg)	58	49	8.2
Vss (mL/kg)	24	89	53

Results

Pharmacokinetics in non-tumor bearing athymic nude mice

The PK profile of anti-DLL4 following a single intravenous (IV) bolus dose in athymic nude mice at doses of 0.2, 2, and 20 mg/kg are shown in **Figure 1** and PK parameters are summarized in **Table 1**. As the dose was increased from 0.2 to 20 mg/kg, area under the serum concentration–time curve extrapolated to infinity (AUCinf) increased in a greater than dose-proportional manner. Total clearance (CLtot) decreased with increasing doses, going from 58 mL/day/kg at the 0.2 mg/kg dose to 8.2 mL/day/kg at the 20 mg/kg dose. The volume of distribution at steady-state (Vss) ranged from 24 to 89 mL/kg at the doses tested. These data suggest that the pharmacokinetics of anti-DLL4 were nonlinear in a dose range of 0.2–20 mg/kg in female athymic nude mice.

Tissue distribution study in athymic nude mice

The tissue distribution of anti-DLL4 was determined by dosing [¹²⁵I]-anti-DLL4 mixed with [¹¹¹In]-anti-DLL4 (tracer) in the absence or presence of an excess amount of unlabeled anti-DLL4 at 2 mg/kg or 20 mg/kg in female athymic nude mice. Measurement of [¹²⁵I]-anti-DLL4 (**Fig. 2A**) and [¹¹¹In] anti-DLL4 (**Fig. 2B**) both showed that plasma radioactivity levels in animals that received only tracer decreased very rapidly within 24 h after dosing and were much lower during the entire course of the study compared with the animals that received both tracer and unlabeled antibody (**Fig. 2**). Plasma radioactivity levels in the 2 mg/kg and 20 mg/kg groups were similar up to 4 h, after which the levels in the 2 mg/kg dropped faster than in the 20 mg/kg group. The 20 mg/kg group showed sustained higher levels of plasma radioactivity for the rest of the 7 d study period (**Fig. 2**). In addition, the serum concentrations of anti-DLL4 obtained by enzyme-linked immunosorbent assays (ELISA) in the PK study were very similar to the plasma concentrations in the radiolabeled antibody study.

The radioactivity was also determined in the various tissues collected. In the tracer alone group at the early time points, increased radioactivity signals were seen in the lung and liver compared with the plasma levels for both [¹²⁵I] and [¹¹¹In], and to a lesser extent in the spleen, kidney and adrenal gland for only [¹¹¹In] (**Fig. 3**). Co-dosing with either 2 mg/kg or 20 mg/kg of unlabeled anti-DLL4 showed significant suppression of the radioactivity uptake ([¹²⁵I] and/or [¹¹¹In]) in these tissues (**Fig. 3**). Some suppression of radioactivity was also seen in the heart tissue with [¹¹¹In]. Both 2 mg/kg and 20 mg/kg reached

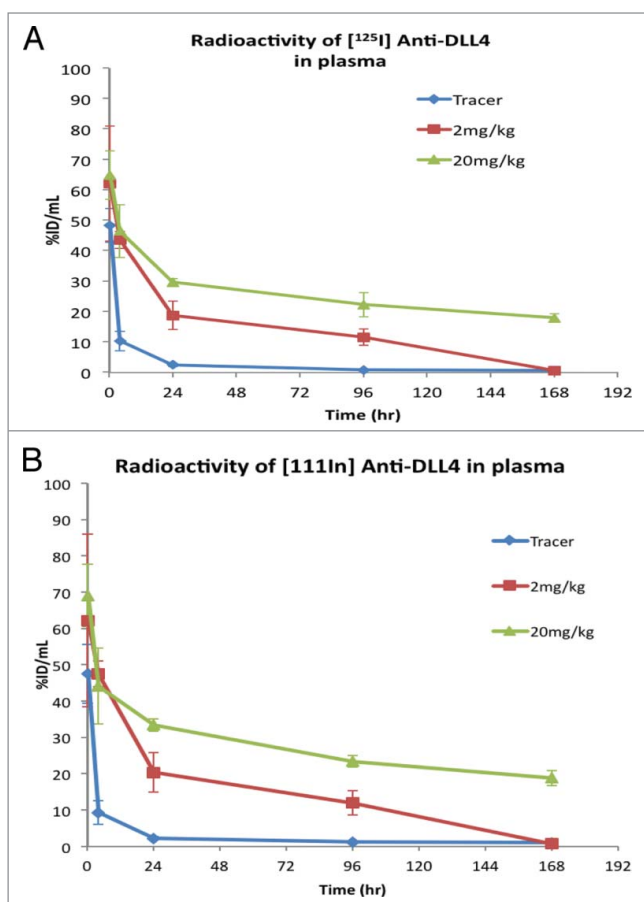


Figure 2. Changes in plasma radioactivity levels (Mean \pm SD, $n = 3$) following IV administration of $[^{125}\text{I}]$ - and $[^{111}\text{In}]$ -labeled anti-DLL4 either as tracer alone or with 2 mg/kg and 20 mg/kg of unlabeled anti-DLL4 in athymic nude mice. (A) Radioactivity of $[^{125}\text{I}]$ anti-DLL4; (B) Radioactivity of $[^{111}\text{In}]$ anti-DLL4.

similar levels of suppression for the first 4 h (Fig. 3), suggesting that 2 mg/kg unlabeled anti-DLL4 was sufficient to saturate binding in these tissues.

To determine whether anti-DLL4 is internalized and degraded in the tissues, the radioactivity signals of $[^{125}\text{I}]$ and $[^{111}\text{In}]$ were compared. $[^{125}\text{I}]$ -labeled antibody reflects tissue uptake kinetics whereas $[^{111}\text{In}]$ -DOTA labeled antibody is a residualizing probe that will accumulate in the cells if the labeled antibody is internalized. Analysis of tissue $[^{125}\text{I}]$ signals showed that after the initial rapid distribution to the lungs and liver in the tracer alone group (Fig. 4A, 4C), $[^{125}\text{I}]$ signals decreased quickly to minimal levels at 24 h and remained at this low level for the rest of study duration. However, the $[^{111}\text{In}]$ signals in the same tissues were maintained at relatively higher levels for a longer duration (Fig. 4B, 4D), suggesting that anti-DLL4 was, at least to some extent, internalized and degraded intracellularly in these tissues.

Anti-tumor efficacy in mice bearing MV522 human lung tumor xenografts

Anti-DLL4 was evaluated for anti-tumor activity in the MV522 human lung tumor model at 6 doses ranging from 1 to

Table 2. Anti-DLL4 exposure and anti-tumor activity in a MV522 human lung tumor xenograft mouse model

Treatment Group	AUCinf (day $\cdot\mu\text{g/mL}$)	Time to Tumor Doubling (day)
Vehicle	—	3.5
Anti-DLL4 – 1 mg/kg	50.5	6
Anti-DLL4 – 10 mg/kg	569	10.5
Anti-DLL4 – 20 mg/kg	1810	10.5
Anti-DLL4 – 30 mg/kg	2660	9.5
Anti-DLL4 – 60 mg/kg	5460	8
Anti-DLL4 – 100 mg/kg	7830	13

100 mg/kg. This model was selected due to its previously characterized sensitivity to anti-DLL4.¹⁸ As shown in Figure 5, a single IV dose of anti-DLL4 showed substantial anti-tumor activity as determined by the time to tumor doubling (TTD) (Table 2). Animals treated with vehicle had tumors that doubled in size in 3.5 d. The TTD increased to 6 d following a single dose of 1 mg/kg of anti-DLL4. A TTD of \sim 10.5 d was achieved at 10 mg/kg with little additional increase observed at higher doses. Estimated AUCinf values at the various doses are shown in Table 2 and represent the total exposure to anti-DLL4 after a single IV dose. For doses from 1 to 100 mg/kg, AUCinf increased more than dose proportionally, indicating that the PK of anti-DLL4 is nonlinear in tumor bearing athymic nude mice.

Discussion

Anti-DLL4 is a unique antibody that binds selectively to DLL4 and was shown to cause significant tumor growth inhibition in several xenograft models tested.^{3,18} Since anti-DLL4 binds to DLL4 proteins in multiple species including mouse and rat, we could explore its activity in various rodent models. To gain a better understanding of the therapeutic potential of anti-DLL4, we assessed its pharmacokinetics and tissue distribution in mouse and anti-tumor activity in xenograft models over a range of doses.

The pharmacokinetics of anti-DLL4 in athymic nude mice, following a single IV dose, appeared to be nonlinear in the dose range of 0.2–20 mg/kg. The nonlinear PK data suggest that the total clearance of anti-DLL4 comprises a specific (target-mediated) CL component and a non-specific CL component, with the specific CL component having a greater contribution at the lower doses. The total clearance decreased with increased dose likely due to saturation of the target. At the highest dose of 20 mg/kg, the clearance value of 8.2 mL/day/kg was similar to the non-specific clearance values in mice seen with typical humanized antibodies (\sim 3–16 mL/day/kg).^{20,21}

We further assessed the tissue distribution of anti-DLL4 in athymic nude mice to determine if any specific tissue distribution could contribute to the nonlinear PK seen with this molecule. The specificity of tissue distribution was determined by assessing whether excess amounts of unlabeled antibody could decrease the tracer distribution to the tissues. To determine whether anti-DLL4 is internalized and intracellularly degraded in the specific target tissue, we used both $[^{125}\text{I}]$ labeled anti-DLL4 and $[^{111}\text{In}]$ labeled anti-DLL4.

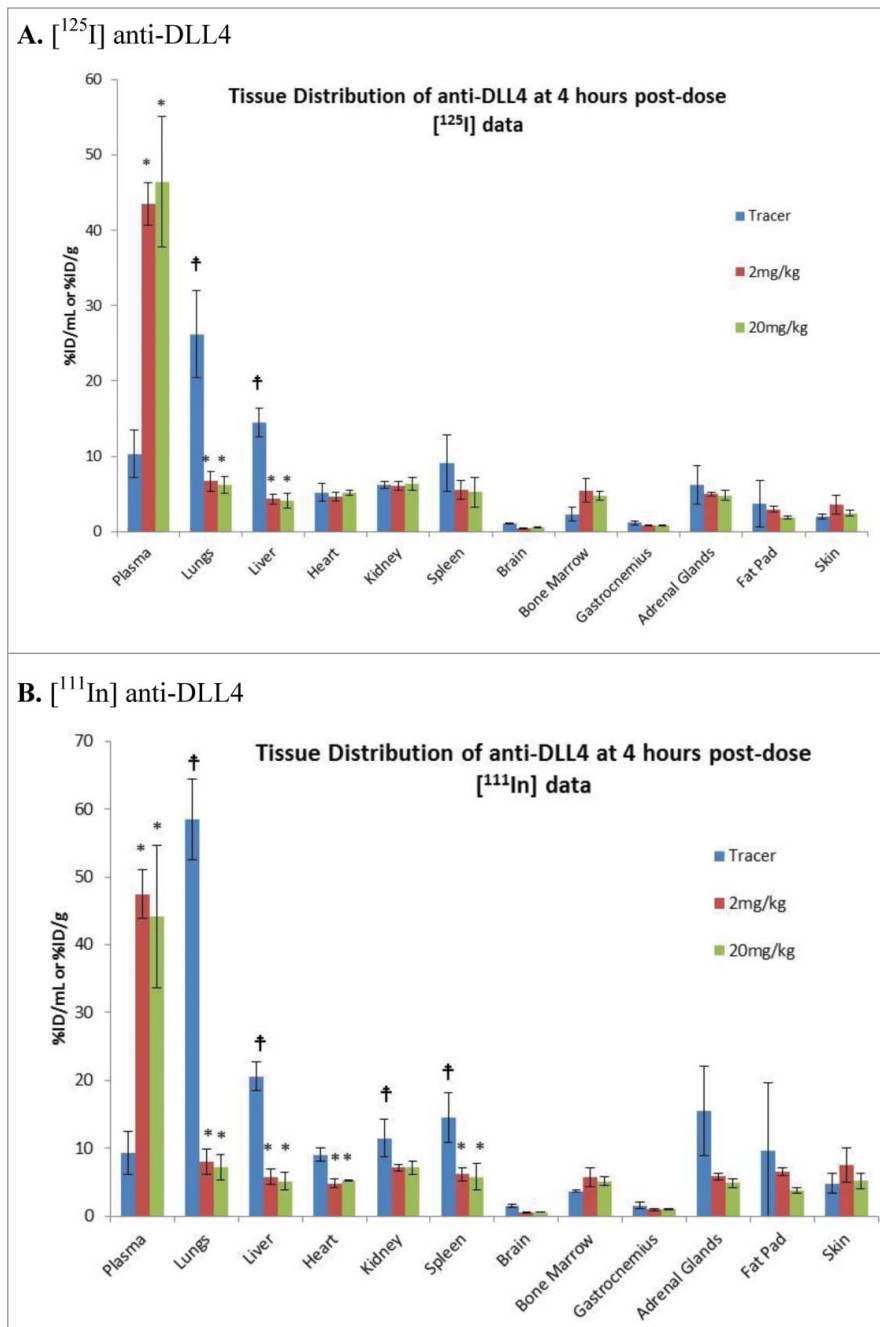


Figure 3. Tissue Distribution of [¹²⁵I]-labeled / [¹¹¹In] anti-DLL4 following administration either as tracer alone or with 2 mg/kg and 20 mg/kg of unlabeled anti-DLL4. Representative tissue data were from 4h post-dosing (Mean ± SD, n = 3 per time point per group). (A) [¹²⁵I] anti-DLL4; (B) [¹¹¹In] anti-DLL4. P values were determined using student *t* test comparing (i) radioactivity in different organs with plasma in the tracer group; (ii) comparing tissue radioactivity in the tracer alone group with that in 2 mg/kg or 20 mg/kg groups. † (for i) and * (for ii) indicates *p* < 0.05.

Though both probes can be used to assess the specific tissue distribution, [¹²⁵I]-labeled antibody reflects tissue uptake kinetics, whereas [¹¹¹In]-DOTA labeled antibody is a residualizing probe that is charged and highly polar, causing it to accumulate in cells if the labeled antibody is internalized. It is known that [¹²⁵I] is released from the antibody quickly as a result of catabolism and the free [¹²⁵I] most likely returns back into the circulation. In contrast, [¹¹¹In] is retained much longer and accumulates in the cells, thus

showing a different kinetic profile relative to the [¹²⁵I] probe.^{22,23} Using these two probes together could help determine if the antibody is internalized and degraded intracellularly.

Our data showed that following dosing with radiolabeled anti-DLL4, plasma radioactivity levels dropped rapidly in the tracer alone group. Co-administration of either 2 mg/kg or 20 mg/kg of unlabeled anti-DLL4 resulted in a similar increase in plasma radioactivity at 15 min and 4 h, suggesting that anti-DLL4 has

specific tissue distribution that can be saturated even at 2 mg/kg. After 24 h however, the plasma radioactivity level in the 2 mg/kg group decreased faster than that in 20 mg/kg group, probably due to the higher concentrations of unlabeled antibody in the 20 mg/kg group that likely maintains receptor saturation over the 7 d study period. The rapid decline of plasma radioactivity levels in the tracer alone group and the dose dependent increase in the plasma radioactivity upon co-administration of unlabeled anti-DLL4 were consistent with the PK results where clearance of anti-DLL4 decreased with an increase in dose. This suggested that anti-DLL4 has specific and saturable tissue distribution that may drive the nonlinearity of its systemic PK.

To identify which tissue (s) may be responsible for the specific distribution of anti-DLL4, tissue radioactivity levels were measured in the same mice. In the tracer alone group, radioactivity levels of [¹²⁵I] and/or [¹¹¹In] increased rapidly in the lung and liver, and to a lesser extent in spleen, kidney and adrenal gland. Co-administration of either 2 mg/kg or 20 mg/kg unlabeled anti-DLL4 significantly decreased radioactivity levels in these tissues, suggesting that anti-DLL4 specifically distributed to these tissues and that the distribution could be saturated by doses of 2 mg/kg and higher. Though the 2 mg/kg dose appeared to suppress tissue radioactivity uptake, the plasma radioactivity levels decreased faster after 24 h relative to the 20 mg/kg dose group. The 20 mg/kg dose group was able to maintain sustained radioactivity levels in the plasma and suppress tissue radioactivity uptake over the 7 d study period, indicating longer saturation than at the lower dose. In the tissues, unlike the [¹²⁵I] signal that decreased after peaking at 4h, the %ID/g from [¹¹¹In] in the tracer alone group was higher than that of [¹²⁵I] at all time-points and increased over the first 24 h followed by a slower decrease when compared with [¹²⁵I]. Since [¹¹¹In]-DOTA is a residualizing probe,²² these data suggest that anti-DLL4 possibly undergoes some degree of internalization and degradation as indicated by the increasing radioactive signal over 24 h.

Anti-DLL4 showed robust anti-tumor activity in a wide range of tumor xenograft models, with some models more dependent

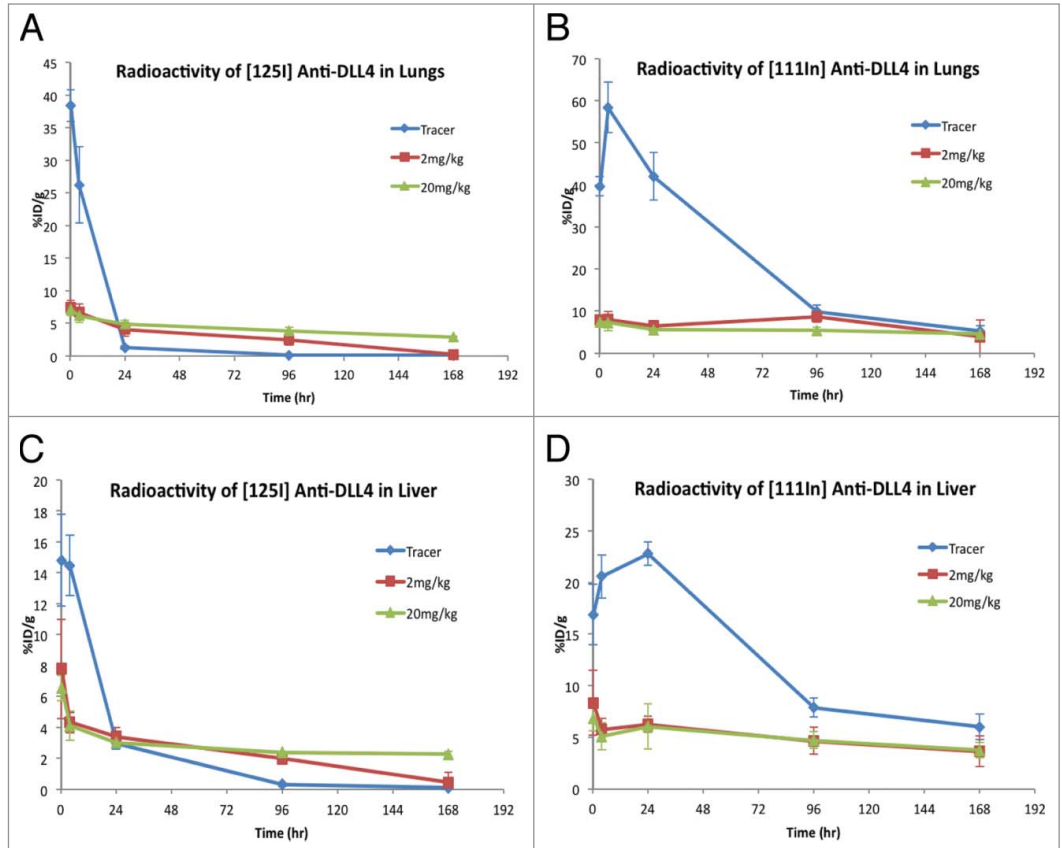


Figure 4. Comparison of distribution of [¹²⁵I]- vs. [¹¹¹In]-anti-DLL4 in the lungs and liver over time following administration either as tracer alone or with 2 mg/kg and 20 mg/kg of unlabeled anti-DLL4. Radioactivity levels were assessed at 15 min, 4 h, 24 h, 4 d, and 7 d (Mean ± SD, n = 3 per time point per group). (A) [¹²⁵I]-anti-DLL4 in lungs; (B) [¹¹¹In]-anti-DLL4 in the lungs; (C) [¹²⁵I]-anti-DLL4 in liver; (D) [¹¹¹In]-anti-DLL4 in the liver.

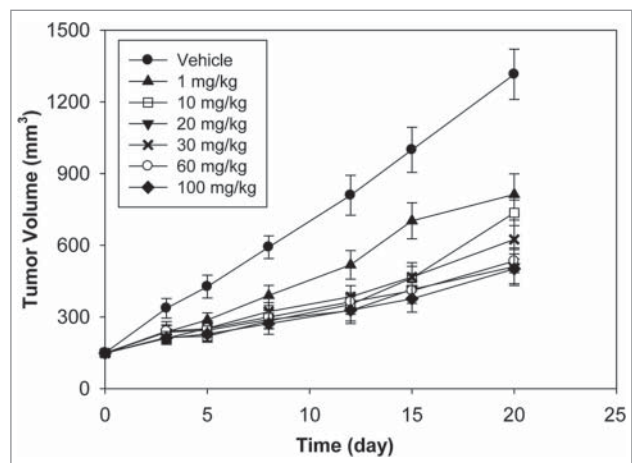


Figure 5. Antitumor efficacy of Anti-DLL4 in MV522 human lung tumor xenograft model after a single IV dose (n = 9/group, mean tumor volume ± SEM for the time that at least half the animals in the group remained on study).

on DLL4.³ MV522 was chosen as a representative model to assess the efficacious dose range due to its previously characterized sensitivity to anti-DLL4.³ Anti-DLL4 showed anti-tumor activity even at the lowest dose tested of 1 mg/kg. Maximal anti-tumor activity was seen at a relatively modest dose of 10 mg/kg with little additional gain at higher doses despite a significant increase in overall exposure (AUCinf). This finding is consistent with the PK profiles and the tissue distribution data that showed saturation of systemic clearance at doses between 2 and 20 mg/kg indicating saturation of any tissue sinks. Since the efficacy studies showed maximal efficacy at 10 mg/kg, it suggests that the antigen in the tumor was likely saturated at a similar dose as in the normal tissues.

In summary, these studies demonstrated that anti-DLL4 had nonlinear PK in mice and rapid and specific distribution to several normal tissues, including the lung, liver, spleen, kidney and adrenal gland. The decrease in clearance with increase in dose suggests the involvement of target-mediated clearance of anti-DLL4 that could be saturated at higher doses. Indeed, the tissue distribution study showed that anti-DLL4 distribution could be saturated by doses as low as 2 mg/kg at the early time points with higher dose levels needed to maintain tissue saturation over longer durations. Consistent with the PK and tissue distribution profiles, maximal efficacy was seen at doses \geq 10 mg/kg of anti-DLL4 when non-tumor tissue sinks were presumably saturated. These findings highlight the importance of mechanistic understanding of antibody disposition to enable dosing strategies for maximizing efficacy.

Materials and Methods

Antibodies

Anti-DLL4 was generated at Genentech Inc. for the in vivo PK, efficacy, and tissue distribution studies. Anti-DLL4 is a phage-derived humanized IgG1 monoclonal antibody that binds selectively to DLL4 from multiple species (mouse, rat, cynomolgus monkey, human) with high affinity.¹⁷

Pharmacokinetic study in athymic nude mice

All in vivo PK, tissue distribution, and anti-tumor efficacy studies were approved by the Institutional Animal Care and Use Committee at Genentech, Inc. and conducted in compliance with the regulations of the Association for Assessment and Accreditation of Laboratory Animal Care. For the PK study, female athymic nude mice received a single IV dose of 0.2, 2, or 20 mg/kg of anti-DLL4 via the tail vein ($n = 15$ /group). Blood samples were collected via retro-orbital bleeds performed on alternating eyes and the terminal blood sample was collected via cardiac stick from each animal in each dosing group at the following time points with three mice per time point: 10 min, 1, 3, 5, 8, and 24 h; and 2, 3, 4, 7, 10, 14, 17, 21, and 28 d. Samples were processed to collect serum for measurement of anti-DLL4 concentrations. Composite serum-concentration time profiles were constructed for pharmacokinetic analysis.

Radiolabeling of anti-DLL4 with Iodine-125 and Indium-111

For tissue distribution studies, anti-DLL4 was radiolabeled separately with either Iodine-125 [¹²⁵I] or Indium-111 [¹¹¹In]. For [¹²⁵I] labeling, the indirect iodination addition method as previously described was used.²⁴ The [¹²⁵I] radiolabeled protein was purified using NAP5TM columns pre-equilibrated in PBS. For [¹¹¹In] labeling, a previously reported method was used.²⁵ Briefly, anti-DLL4 was conjugated with DOTA (1,4,7,10-tetraazacyclododecane-N,N',N'',N'''-tetraacetic acid) and [¹¹¹In] was incorporated into DOTA. The radiolabeled antibodies were shown to maintain comparable antigen binding to its unmodified counterparts by ELISA and were shown to be intact by size-exclusion HPLC with no evidence of aggregation or degradation. The specific activity for [¹²⁵I] labeled antibody was 14.13 μ Ci/ μ g and the specific activity for [¹¹¹In] labeled antibody was 13.16 μ Ci/ μ g.

Tissue distribution study in athymic nude mice

Female athymic nude mice ($n = 15$ /group) received a single IV dose of radiolabeled anti-DLL4 ([¹²⁵I]-anti-DLL4 mixed with [¹¹¹In]-anti-DLL4 at 200 μ Ci/kg each), either alone (tracer group) or along with unlabeled anti-DLL4 at 2 mg/kg or 20 mg/kg. All animals received an intraperitoneal injection of 30 mg/kg sodium iodide at 1 and 24 h before dosing to prevent [¹²⁵I] sequestration to the thyroid. Following dosing, blood samples were taken at 15 min, 4 h, 1, 4, and 7 d ($n = 3$ per time point in each group) via retro-orbital bleed and processed for plasma. Various tissues were also harvested from these animals at the same time points ($n = 3$ per time point in each group), including liver, lungs, kidneys, heart, spleen, brain, bone marrow, gastrocnemius, adrenal glands, fat pad and skin. The radioactivity levels in plasma and tissues were measured using a gamma counter and expressed as percentage of injected dose per mL or per gram of sample (%ID/mL or %ID/g). P values were determined using student *t* test comparing (i) the radioactivity in different organs with that in plasma in the tracer group, and (ii) tissue radioactivity in the tracer alone group with that in 2 mg/kg or 20 mg/kg groups, respectively. P value < 0.05 is defined as significantly different.

Anti-tumor efficacy study in mice bearing MV522 human lung tumor xenografts

Female athymic nude mice were each injected with 10 million human lung carcinoma MV522 cells, subcutaneously in the right dorsal flank. The MV522 cells were obtained from cultures grown at Piedmont Research Center (original source: Dr. Kelner from University of California at San Diego) and cultured in RPMI 1640 supplemented with 10% fetal bovine serum and 2 mM L-glutamine. When tumors reached a volume range of 70–210 mm³, mice were randomized into seven groups ($n = 9$ per group) and received a single IV dose of phosphate buffered saline (vehicle control group) or anti-DLL4 (treatment groups) at doses of 1, 10, 20, 30, 60, or 100 mg/kg. For each group, blood samples were collected from the retro-orbital sinuses of 3 mice per time point at 4 h and 1, 3, 7, 14, and 21 d post dose and

processed for serum for measurement of anti-DLL4 concentrations. Composite serum-concentration time profiles were constructed for pharmacokinetic analysis. Tumors were measured twice each week for the duration of the study and tumor volume was calculated using the following formula: Tumor Volume (mm^3) = (length \times width²) \times 0.5. The results were shown as mean tumor volume \pm standard error of the mean (SEM) for the time that at least half the animals in the group remained on study. TTD was calculated and is defined as the time in days for a tumor to double in volume from the day of randomization.

Bioanalysis of serum and plasma samples

Serum samples from the PK and efficacy studies were analyzed for anti-DLL4 concentrations using a quantitative ELISA. A DLL4 extracellular domain protein with a histidine tag was used as the capture reagent and goat anti-human IgG1-Fc-horseradish peroxidase as the detection reagent. The minimum quantifiable concentration was 1.6 ng/mL in the PK study and 0.65 ng/mL in the efficacy study.

Pharmacokinetic Data Analysis

Serum concentration-time profiles from the PK and efficacy studies were used to estimate the following PK parameters in

mouse using non-compartmental analysis (WinNonlin, Pharsight Corporation, Mountain View, CA): total drug exposure defined as area under the serum concentration–time curve extrapolated to infinity (AUC_{inf}), total clearance (CL_{tot}), volume of distribution at steady-state (V_{ss}), and observed maximum serum concentration (C_{max}). A naïve pooled approach (combining data from all animals in each dose group) was used to provide one estimate of each parameter for each dose group.

Disclosure of Potential Conflicts of Interest

All authors are current or past employees of Genentech, a member of the Roche Group, and hold financial interest in Hoffmann-La Roche.

Acknowledgments

We thank the In Vivo Studies Group at Genentech for conducting the mouse PK and tissue distribution studies.

Funding

All financial support was provided by Genentech.

References

- Bray SJ. Notch signalling: a simple pathway becomes complex. *Nat Rev Mol Cell Biol* 2006; 7:678-89; PMID:16921404; <http://dx.doi.org/10.1038/nrm2009>
- Artavanis-Tsakonas S, Rand MD, Lake RJ. Notch signaling: cell fate control and signal integration in development. *Science* 1999; 284:770-6; PMID:10221902; <http://dx.doi.org/10.1126/science.284.5415.770>
- Yan M, Plowman GD. Delta-like 4/Notch signaling and its therapeutic implications. *Clin Cancer Res* 2007; 13:7243-6; PMID:18094402; <http://dx.doi.org/10.1158/1078-0432.CCR-07-1393>
- Yan M. Therapeutic promise and challenges of targeting DLL4/NOTCH1. *Vasc Cell* 2011; 3:17; PMID:21824400; <http://dx.doi.org/10.1186/2045-824X-3-17>
- Kuhnert F, Kirshner JR, Thurston G. Dll4-Notch signaling as a therapeutic target in tumor angiogenesis. *Vasc Cell* 2011; 3:20; PMID:21923938; <http://dx.doi.org/10.1186/2045-824X-3-20>
- Hofmann JJ, Iruela-Arispe ML. Notch signaling in blood vessels: who is talking to whom about what? *Circ Res* 2007; 100:1556-68; PMID:17556669; <http://dx.doi.org/10.1161/01.RES.0000266408.42939.e4>
- Iso T, Hamamori Y, Kedes L. Notch signaling in vascular development. *Arterioscler Thromb Vasc Biol* 2003; 23:543-53; PMID:12615665; <http://dx.doi.org/10.1161/01.ATV.0000060892.81529.8F>
- Gale NW, Dominguez MG, Noguera I, Pan L, Hughes V, Valenzuela DM, Murphy AJ, Adams NC, Lin HC, Holash J, et al. Haploinsufficiency of delta-like 4 ligand results in embryonic lethality due to major defects in arterial and vascular development. *Proc Natl Acad Sci U S A* 2004; 101:15949-54; PMID:15520367; <http://dx.doi.org/10.1073/pnas.0407290101>
- Duarte A, Hirashima M, Benedito R, Trindade A, Diniz P, Bekman E, Costa L, Henrique D, Rossant J. Dosage-sensitive requirement for mouse Dll4 in artery development. *Genes Dev* 2004; 18:2474-8; PMID:15466159; <http://dx.doi.org/10.1101/gad.1239004>
- Krebs LT, Shutter JR, Tanigaki K, Honjo T, Stark KL, Gridley T. Haploinsufficient lethality and formation of arteriovenous malformations in Notch pathway mutants. *Genes Dev* 2004; 18:2469-73; PMID:15466160; <http://dx.doi.org/10.1101/gad.1239204>
- Mailhos C, Modlich U, Lewis J, Harris A, Bicknell R, Ish-Horowicz D. Delta4, an endothelial specific notch ligand expressed at sites of physiological and tumor angiogenesis. *Differentiation* 2001; 69:135-44; PMID:11798067; <http://dx.doi.org/10.1046/j.1432-0436.2001.690207.x>
- Rao PK, Dorsch M, Chickering T, Zheng G, Jiang C, Goodearl A, Kadesch T, McCarthy S. Isolation and characterization of the notch ligand delta4. *Exp Cell Res* 2000; 260:379-86; PMID:11035934; <http://dx.doi.org/10.1006/excr.2000.5034>
- Shutter JR, Scully S, Fan W, Richards WG, Kitajewski J, Deblandre GA, Kintner CR, Stark KL. Dll4, a novel Notch ligand expressed in arterial endothelium. *Genes Dev* 2000; 14:1313-8; PMID:10837024
- Jakobsson L, Bentley K, Gerhardt H. VEGFRs and Notch: a dynamic collaboration in vascular patterning. *Biochem Soc Trans* 2009; 37:1233-6; PMID:19909253; <http://dx.doi.org/10.1042/BST0371233>
- Jakobsson L, Franco CA, Bentley K, Collins RT, Ponsioen B, Aspalter IM, Rosewell I, Busse M, Thurston G, Medvinsky A, et al. Endothelial cells dynamically compete for the tip cell position during angiogenic sprouting. *Nat Cell Biol* 2010; 12:943-53; PMID:20871601; <http://dx.doi.org/10.1038/ncb2103>
- van Es JH, van Gijn ME, Riccio O, van den Born M, Vooijs M, Begthel H, Cozijnsen M, Robine S, Winton DJ, Radtke F, et al. Notch/gamma-secretase inhibition turns proliferative cells in intestinal crypts and adenomas into goblet cells. *Nature* 2005; 435:959-63; PMID:15959515; <http://dx.doi.org/10.1038/nature03659>
- Yan M, Callahan CA, Beyer JC, Allamneni KP, Zhang G, Ridgway JB, Niessen K, Plowman GD. Chronic DLL4 blockade induces vascular neoplasms. *Nature* 2010; 463:E6-7; PMID:20147986; <http://dx.doi.org/10.1038/nature08751>
- Ridgway J, Zhang G, Wu Y, Stawicki S, Liang WC, Chantry Y, Kowalski J, Watts RJ, Callahan C, Kasman I, et al. Inhibition of Dll4 signalling inhibits tumour growth by deregulating angiogenesis. *Nature* 2006; 444:1083-7; PMID:17183323; <http://dx.doi.org/10.1038/nature05313>
- Shutter JR, Scully S, Fan W, Richards WG, Kitajewski J, Deblandre GA, Kintner CR, Stark KL. Dll4, a novel Notch ligand expressed in arterial endothelium. *Genes Dev* 2000; 14:1313-8; PMID:10837024
- Deng R, Iyer S, Theil FP, Mortensen DL, Fielder PJ, Prabhu S. Projecting human pharmacokinetics of therapeutic antibodies from nonclinical data: what have we learned? *MAbs* 2011; 3:61-6; PMID:20962582; <http://dx.doi.org/10.4161/mabs.3.1.13799>
- Kamath AV, Lu D, Gupta P, Jin D, Xin Y, Brady A, Stephan JP, Li H, Tien J, Qing J, et al. Preclinical pharmacokinetics of MFGR1877A, a human monoclonal antibody to FGFR3, and prediction of its efficacious clinical dose for the treatment of t(4;14)-positive multiple myeloma. *Cancer Chemother Pharmacol* 2012; 69:1071-8; PMID:22203368; <http://dx.doi.org/10.1007/s00280-011-1807-5>
- Boswell CA, Bumbaca D, Fielder PJ, Khawli LA. Compartmental tissue distribution of antibody therapeutics: experimental approaches and interpretations. *AAPS J* 2012; 14:612-8; PMID:22648903; <http://dx.doi.org/10.1208/s12248-012-9374-1>
- Kobayashi H, Kao CH, Kreitman RJ, Le N, Kim MK, Brechbiel MW, Paik CH, Pastan I, Carrasquillo JA. Pharmacokinetics of 111In- and 125I-labeled antiTac single-chain Fv recombinant immunotoxin. *J Nucl Med* 2000; 41:755-62; PMID:10768579
- Chizzonite R, Truitt T, Podlaski FJ, Wolitzky AG, Quinn PM, Nunes P, Stern AS, Gately MK. IL-12: monoclonal antibodies specific for the 40-kDa subunit block receptor binding and biologic activity on activated human lymphoblasts. *J Immunol* 1991; 147:1548-56; PMID:1715362
- Bumbaca D, Xiang H, Boswell CA, Port RE, Stainton SL, Mundo EE, Ulufatu S, Bagri A, Theil FP, Fielder PJ, et al. Maximizing tumour exposure to anti-neuropilin-1 antibody requires saturation of non-tumour tissue antigenic sinks in mice. *Br J Pharmacol* 2012; 166:368-77; PMID:22074316; <http://dx.doi.org/10.1111/j.1476-5381.2011.01777.x>